Analysis of Turbulent Pipe Flow with a Variable Heat Transfer Coefficient Using Integral Equations

Jim Beale* and Brian Vick†
Virginia Polytechnic Institute and State University, Blacksburg, Virginia

A solution methodology is developed to investigate the problem of heat transfer to fully developed turbulent flow in a pipe subject to a variable external heat transfer coefficient. The variable convection coefficient serves to model a tube fitted with an array of external fins. The solution technique consists of using a Green's function to derive a singular Volterra integral equation for the wall temperature, which is then resolved using a standard integration scheme with the aid of singularity subtraction. The technique provides a straightforward combination of analytical and numerical methods which can handle a large class of problems involving variable boundary condition parameters. The method is used to present a parameter study displaying the effects of the variation of the heat transfer coefficient, the Reynolds number, and the Prandtl number on the heat transfer in turbulent pipe flow.

Nomenclature

C_f = friction factor
$f(\xi)$ = function defined by Eq. (10c)
$g(\eta)$ = dimensionless eddy diffusivity
G = Green's function
$h(z)$ = external heat transfer coefficient
$H(\xi)$ = dimensionless heat transfer coefficient
H_o = constant heat transfer coefficient
k = thermal conductivity
K = kernel defined by Eq. (10b)
Nu = Nusselt number
Pe = Péclét number
Pr = Prandtl number
Pr_t = turbulent Prandtl number
$Q(\xi)$ = total heat transfer, $1-\theta_b(\xi)$
r = radial variable
r_o = tube radius
Re = Reynolds number
Re* = Re $\sqrt{C_f/2}$, Reynolds number based on u^*
$S(\eta,\xi)$ = heat source term
$T(r,z)$ = mean temperature
T_o = inlet temperature
T_∞ = ambient temperature
$u(r)$ = mean velocity profile
u^* = friction velocity, $\sqrt{\tau_w/\rho}$
u^+ = dimensionless velocity, u/u^*
u_b = bulk velocity
$v(\eta)$ = dimensionless velocity profile, u/u_b
z = axial variable
α = thermal diffusivity
δ = delta function
ε_H = eddy diffusivity
ε_m = eddy viscosity
η = dimensionless radial variable
$\theta(\eta,\xi)$ = dimensionless temperature
$\theta_b(\xi)$ = dimensionless bulk temperature
$\theta_w(\xi)$ = dimensionless wall temperature
λ_m = eigenvalue
ν = viscosity
ξ = dimensionless axial variable
τ_w = wall shear stress
$\psi_m(\eta)$ = eigenfunction

Received March 9, 1987; revision received Aug. 7, 1987.

*Assistant Professor, Mechanical Engineering Department.
†Assistant Professor, Mechanical Engineering Department. Member AIAA.

Introduction

THIS paper describes a theoretical investigation of the effect of an axially varying external convection coefficient on the heat transfer characteristics in a fully developed turbulent pipe flow. One of the main difficulties inherent in such a study is the description of the turbulence itself. Since there are no exact methods for calculating turbulent velocity and temperature distributions at the present time, we must resort to turbulence modeling. In this analysis, the model of Travis et al.[1] is employed. This model is the most accurate available for smooth pipe flow since it satisfies all analytical contraints and matches the best available experimental data.

Another major difficulty is associated with the axial variation of the convection coefficient. The variable boundary condition parameter causes the governing energy equation to become nonseparable. As a result, all standard analytical techniques, such as the Green's function or the finite-integral transform technique, fail when applied to a problem with a variable boundary condition parameter. This is why such an important problem, with many practical applications, remains relatively untouched.

There has been a great deal of research into heat transfer to a turbulent pipe flow, however all studies have concentrated on a specified wall temperature or a specified wall heat flux. Martinelli[2] studied the case of constant wall temperature for heat transfer to turbulent flow of a molten metal. Sleicher and Tribus[3] solved the case of a step change in wall temperature and showed how this solution can be extended to solve the cases of an arbitrary wall temperature distribution and a uniform wall heat flux. In a three-paper exposition, Notter et al.[4-6] used the method of matched asymptotic expansions to solve the turbulent Graetz problem for the cases of uniform wall temperature and uniform wall heat flux. Shibani and Özisik[7] considered turbulent flow between parallel plates using the matched asymptotic expansion technique. Siegel and Sparrow[8] studied the effects of internal heat sources and a specified wall heat flux in turbulent flow in a circular tube. Apparently, no one has considered the convective boundary condition in turbulent pipe flow.

A few studies have been conducted on heat transfer to laminar pipe flow with a variable convective boundary. Sparrow and Charmchi[9] used a finite-difference scheme to solve the Graetz problem for a stepwise periodic variation of the heat transfer coefficient. However, the discontinuous nature of the boundary condition made the computational task quite de-

manding, so that a complete parameter study was not possible. Vick and Wells[10] employed a variable eigenvalue technique to study laminar flow with an axially varying heat transfer coefficient. Recently, Vick et al.[11] used integral equations to analyze an arbitrary variation of the heat transfer coefficient in laminar flow and applied their results to both a stepwise periodic and harmonic variation.

There are many applications where the axial variation of the external convection coefficient is significant. An important example is the heat transfer enhancement due to external fins. Since a fin increases the effective coefficient of heat exchange between the fin base and the ambient, a duct fitted with an array of external fins can be modeled as an unfinned duct with a periodically low and high value of the heat transfer coefficient, corresponding to unfinned and finned regions, respectively. This model suggests a stepwise periodic heat transfer coefficient. However, the effect of axial conduction in the wall may smooth out the stepwise nature of the convection coefficient and a harmonic variation may also be appropriate.

The present investigation presents a solution methodology for heat transfer to a turbulent pipe flow for an arbitrary variation of the external heat transfer coefficient. The solution is developed in terms of an arbitrary mean velocity profile and eddy diffusivity. The model of Travis et al.[1] is then used to describe the turbulence. The standard Green's function technique is used to convert the governing equations into a singular Volterra integral equation which is then resolved by a standard numerical integration procedure. Results are presented for constant, stepwise, and harmonic variations of the external convection coefficient. A parameter study is presented showing the effect of Re and Pr on the heat transfer characteristics.

Mathematical Model

Flowfield

In order to solve the thermal energy equation, it is necessary to have an adequate description of the turbulence. In the usual way, the dependent variables in the axisymmetric momentum equation are expressed as a sum of mean and fluctuating components. The momentum equation is then time-averaged and for fully developed conditions reduces to the following

$$\frac{r}{r_o}u^{*2} = -\nu\frac{du}{dr} + \overline{u'v'} \tag{1}$$

The Reynold's stress, $\rho\overline{u'v'}$, is expressed as a turbulent shear stress through an eddy viscosity as

$$\overline{u'v'} = -\varepsilon_m\frac{du}{dr} \tag{2}$$

Then, assuming that an appropriate relation exists for ε_m, Eq. (1) can be integrated and expressed in terms of dimensionless variables as

$$u^+ = 0.5\,\mathrm{Re}^*\int_\eta^1 \frac{\eta\,d\eta}{(\varepsilon_m/\nu+1)} \tag{3}$$

Now, due to the closure problem, it is necessary to resort to an empirical formula for ε_m.

In the paper by Travis et al.[1], Riechardt's two-region eddy viscosity model[12] is modified so that the eddy viscosity and the resulting velocity profile satisfy the following constraints:

1) The eddy viscosity must vanish with the cube of the distance from the wall.

2) The eddy viscosity must be a smooth function of radial position.

3) The velocity gradient must vanish at the pipe center.

4) The continuity equation must be satisfied by the mean velocity.

5) Values of the wall shear stress should follow the accepted friction factor vs Reynolds number relationship, thus Re* follows directly from Re.

6) Point values of the velocity should agree with the best available experimental data.

7) The predicted ratio of bulk velocity to maximum velocity should fit the experimental data.

The eddy viscosity satisfying the above constraints is expressed as

$$\frac{\varepsilon_m}{\nu} = b\left[y^+ - A\tanh\left(\frac{y^+}{A}\right)\right], \qquad y^+ < y_i^+$$

$$= \frac{b}{6}\frac{\mathrm{Re}^*}{2}[1-(F\eta)^2]\left[\frac{2}{3}+2(F\eta)^2\right], \qquad \eta < \eta_i \tag{4}$$

where

$$y^+ = \frac{\mathrm{Re}^*}{2}(1-\eta)$$

The coefficients y_i^+, F, A, and b are presented in the form of polynomial spline functions in terms of Re in the range 4000 to 5.0×10^6, as tabulated in Ref. 1. The velocity profile is then obtained by numerical integration using Eq. (3).

Temperature Field

In a completely analogous way, the temperature in a turbulent pipe flow is expressed as the sum of mean and fluctuating quantities and the energy equation is then time-averaged. The contribution of the turbulence survives the time-averaging process in the term $\overline{v'T'}$, which is expressed as a turbulent heat flux through an eddy diffusivity for heat in the form

$$\overline{v'T'} = -\varepsilon_H\frac{\partial T}{\partial r}$$

A turbulent Prandtl number can then be defined as

$$\mathrm{Pr}_t = \frac{\varepsilon_m}{\varepsilon_H}$$

Since the mechanisms for turbulent transport of momentum and heat are postulated to be the same, Pr_t is usually taken as a constant with values in the range of 0.7 to 1.0. There is some disagreement regarding the most appropriate value since Pr_t actually has some variation across the flow channel, especially near the wall, and also depends on the thermal boundary condition at the wall. However, a constant value of $\mathrm{Pr}_t = 0.9$ has been found to correlate well with experimental data and is used here.

The time-averaged energy equation, with appropriate boundary conditions, can now be expressed in dimensionless form as

$$\frac{v(\eta)}{2}\frac{\partial\theta}{\partial\xi} = \frac{1}{\eta}\frac{\partial}{\partial\eta}\left[\eta g(\eta)\frac{\partial\theta}{\partial\eta}\right] + S(\eta,\xi) \tag{5a}$$

$$\frac{\partial\theta}{\partial\eta} = 0, \qquad \eta = 0 \tag{5b}$$

$$\frac{\partial\theta}{\partial\eta} + H(\xi)\theta = 0, \qquad \eta = 1 \tag{5c}$$

$$\theta = 1, \qquad \xi = 0 \tag{5d}$$

The various dimensionless quantities are defined as follows

$$\eta = \frac{r}{r_o}, \qquad \xi = z/(r_o\mathrm{Pe}) \tag{6a}$$

$$\mathrm{Re} = \frac{2r_o u_b}{\nu}, \qquad \mathrm{Pr} = \frac{\nu}{\alpha}, \qquad \mathrm{Pe} = \mathrm{Re}\cdot\mathrm{Pr} \tag{6b}$$

$$v(\eta) = \frac{u(r)}{u_b} = \frac{\mathrm{Re}^*}{\mathrm{Re}} u^+, \qquad g(\eta) = 1 + \frac{\mathrm{Pr}}{\mathrm{Pr}_t} \cdot \frac{\varepsilon_m}{\nu} \tag{6c}$$

$$H(\xi) = \frac{h(z) r_o}{k} \tag{6d}$$

$$\theta(\eta,\xi) = \frac{T(r,z) - T_\infty}{T_o - T_\infty} \tag{6e}$$

This set of equations models the thermal entry region in a pipe with a fully developed turbulent flow entering at a uniform temperature T_o. A source term $S(\eta,\xi)$ is included to allow for heat generation or viscous dissipation. The fluid exchanges heat with an external environment at temperature T_∞ by virtue of an axially varying heat transfer coefficient $h(z)$. The parameter $h(z)$ allows for the modeling of various situations of engineering interest, including the effect of a nonuniform external flow which varies along the axis of the pipe, or the effect of heat transfer enhancement due to external finning. The difficulty with a variable boundary condition parameter is that it makes the problem nonseparable so that the standard analytical techniques fail. In the next section, a straightforward method for handling an arbitrary variation of the dimensionless coefficient $H(\xi)$ will be developed.

Analysis

The system of Eq. (5) for the developing temperature profile is now solved by employing the Green's function technique to convert the original partial differential equation and boundary conditions into a singular Volterra integral equation for the temperature of the fluid at the wall.

A Green's function is chosen which is governed by the following system of equations

$$\frac{v(\eta)}{2}\frac{\partial G}{\partial \xi} = \frac{1}{\eta}\frac{\partial}{\partial \eta}\left[\eta g(\eta)\frac{\partial G}{\partial \eta}\right] + \delta^r(\eta - \eta_o)\delta(\xi - \xi_o), \qquad 0 \le \eta < 1,\ \xi > 0 \tag{7a}$$

$$\frac{\partial G}{\partial \eta} = 0, \qquad \eta = 0 \tag{7b}$$

$$\frac{\partial G}{\partial \eta} + H_o G = 0, \qquad \eta = 1 \tag{7c}$$

$$G = 0, \qquad \xi < \xi_o \tag{7d}$$

where the Green's function, $G = G(\eta,\xi \mid \eta_o,\xi_o)$, is the response function to a concentrated heat source located at (η_o,ξ_o). The arguments are written to emphasize their effect/cause relationship.

An important feature of this choice of the Green's function is that the boundary condition at $\eta = 1$ is taken with a constant heat transfer coefficient H_o. Thus, the solution to Eq. (7) can be obtained by the finite integral transform technique.[13] Since we have concentrated on pipe flow, the delta function in the radial variable must be taken as a cylindrical delta function.

Following the procedure given in Ozisik,[13] the general solution to the system of Eq. (5) can be expressed in terms of the Green's function as follows:

$$\theta(\eta,\xi) = \int_{\xi_o=0}^{\xi} g(1)\,[H_o - H(\xi_o)]G(\eta,\xi \mid 1,\xi_o)\theta(1,\xi_o)\,d\xi_o + \int_{\eta_o=0}^{1} \eta_o \frac{v(\eta_o)}{2} G(\eta,\xi \mid \eta_o,0)\,d\eta_o + \int_{\xi_0=0}^{\xi}\int_{\eta_o=0}^{1} \eta_o G(\eta,\xi \mid \eta_o,\xi_o)S(\eta_o,\xi_o)\,d\eta_o\,d\xi_o \tag{8}$$

The first integral represents the effect of the heat transfer at the wall due to the variable convection coefficient, the second integral represents the effect of the inlet temperature, and the third integral arises from the source term.

Since $\theta(1,\xi_o)$ in the first integral is still unknown, Eq. (8) is evaluated at $\eta = 1$ and the result is expressed in the form

$$\theta_w(\xi) = \int_{\xi_o=0}^{\xi} K(\xi,\xi_o)\theta_w(\xi_o)\,d\xi_o + f(\xi) \tag{9}$$

where

$$\theta_w(\xi) = \theta(1,\xi) \tag{10a}$$

$$K(\xi,\xi_o) = g(1)\,[H_o - H(\xi_o)]G(1,\xi \mid 1,\xi_o) \tag{10b}$$

$$f(\xi) = \int_{\eta_o=0}^{1} \eta_o \frac{v(\eta_o)}{2} G(1,\xi \mid \eta_o,0)\,d\eta_o + \int_{\xi_o=0}^{\xi}\int_{\eta_o=0}^{1} \eta_o G(1,\xi \mid \eta_o,\xi_o)S(\eta_o,\xi_o)\,d\eta_o\,d\xi_o \tag{10c}$$

have been defined for convenience.

Equation (9) is a Volterra integral equation of the second kind for the surface temperature which can be resolved using a suitable numerical integration technique. However, direct numerical integration is impossible since the kernel $K(\xi,\xi_o)$ is singular when its arguments are equal. The singularity arises from the Green's function at the point where the concentrated heat source is located. Since the Green's function is the response function to the concentrated heat source, it becomes unbounded at that point.

To overcome this difficulty the following singularity subtraction procedure is used to rewrite Eq. (9) as

$$\theta_w(\xi) = \int_{\xi_o=0}^{\xi-\Delta\xi} K(\xi,\xi_0)\theta_w(\xi_o)\,d\xi_o + \int_{\xi_o=\xi-\Delta\xi}^{\xi} K(\xi,\xi_o)[\theta_w(\xi_o) - \theta_w(\xi)]\,d\xi_o + \theta_w(\xi)\int_{\xi_o=\xi-\Delta\xi}^{\xi} K(\xi,\xi_o)\,d\xi_o + f(\xi) \tag{11}$$

where $\Delta\xi$ is the step size used in the numerical integration. Equation (11) is now in a form suitable for direct numerical integration. The integrand in the first integral contains all bounded values, hence provides no difficulties. The integrand in the second integral vanishes at the upper limit of integration, successfully cancelling the singular point of the kernel. The third integral in Eq. (11) contains only the kernel which, although singular, is integrable with analytical expressions available for many variations of the convection coefficient. If an analytical expression is not available, an open numerical integration formula, which avoids the singular point, may be used. Also, since the contribution of the third integral grows increasingly smaller as $\Delta\xi$ decreases, this integral may be neglected for $\Delta\xi$ appropriately small.

Once values for the wall temperature are available, the bulk temperature can immediately be obtained from a numerical integration of the following energy balance

$$\theta_b(\xi) = 1 - 4\int_{\xi'=0}^{\xi} H(\xi')\theta_w(\xi')\,d\xi' + 4\int_{\xi'=0}^{\xi}\int_{\eta=0}^{1} \eta S(\eta,\xi')\,d\eta\,d\xi' \tag{12}$$

Another quantity of interest is the total heat transfer, which in the absence of energy sources ($S = 0$) is given by

$$Q(\xi) = 1 - \theta_b(\xi) = \frac{T_o - T_b}{T_o - T_\infty} \tag{13}$$

The quantity $Q(\xi)$ is the heat transferred from the fluid at some axial location divided by the total heat transferred as thermal saturation is reached. As a result, this particular choice of dimensionless heat transfer is quite relevant for displaying the heat transfer enhancement due to finning but will display an unusual Re dependence, as elaborated in Fig. 7 in the following section. The Nusselt number or internal heat transfer coefficient can be expressed as

$$\mathrm{Nu} = \frac{2H(\xi)\theta_w(\xi)}{\theta_b(\xi) - \theta_w(\xi)} \tag{14}$$

The Green's function, as governed by Eq. (7), is readily resolved by the finite integral transform technique[13] in the form

$$G(\eta,\xi \mid \eta_o,\xi_o) = \sum_{m=1}^{\infty} \psi_m(\eta)\psi_m(\eta_o) \exp[-\lambda_m^2(\xi - \xi_o)] \tag{15}$$

The eigenvalues λ_m and eigenfunctions $\psi_m(\eta)$ are determined from the solutions of the following problem

$$\frac{\mathrm{d}}{\mathrm{d}\eta}\left[\eta g(\eta)\frac{\mathrm{d}\psi_m}{\mathrm{d}\eta}\right] + \lambda_m^2 \eta \frac{v(\eta)}{2}\psi_m(\eta) = 0 \tag{16a}$$

$$\frac{\mathrm{d}\psi_m}{\mathrm{d}\eta} = 0, \qquad \eta = 0 \tag{16b}$$

$$\frac{\mathrm{d}\psi_m}{\mathrm{d}\eta} + H_o\psi_m = 0, \qquad \eta = 1 \tag{16c}$$

The eigenfunctions have been normalized so that

$$\int_{\eta=0}^{1} \eta \frac{v(\eta)}{2}\psi_m^2(\eta)\,\mathrm{d}\eta = 1 \tag{17}$$

The value of H_o may be chosen arbitrarily. For the special case of $H_o = 0$, the eigenvalues correspond to those for a specified heat flux[5,8] whereas for the case $H_o \to \infty$, the eigenvalues correspond to those appropriate for a specified wall temperature.[3,4] However, in order to use the eigenvalues and eigenfunctions computed in previous works, the turbulence model must be the same since it directly influences $g(\eta)$ and $v(\eta)$. A logical choice for H_o is a value which makes the kernel K in Eq. (11) as small as possible. In this way, a smaller portion of the solution must be resolved by a numerical integration and a larger portion will be contained in the function $f(\xi)$ defined by Eq. (10c). In fact, for the special case $H(\xi) = H_o$, the kernel defined by Eq. (10b) vanishes and Eqs. (8) and (9) reduce to the exact analytical solution.

The solution of this eigenvalue problem could be attempted by the method of matched asymptotic expansions for simplified versions of the velocity profile and eddy diffusivity.[4-7] However, due to the numerically integrated velocity profile, it becomes impractical to use asymptotic analysis and a numerical approach must be adopted.

The differential equation given by Eq. (16a) is integrated from $\eta = 0$ to $\eta = 1$ by Butcher's (5), (6) method[14] using an approximate value for the eigenvalue λ_m. The standard "shooting method" is employed with the boundary condition at $\eta = 1$ providing the convergence criterion, since this will be satisfied exactly if λ_m is exact. This procedure was tested with $v(\eta) = 2$, $g(\eta) = 1$, which yields the precisely known Bessel functions. The error of $\psi_m(1)$ is less than 1% for the first 50 eigenvalues, while the eigenvalues themselves are within 0.001% of their correct value. The accuracy is expected to be of the same order in the case of turbulent flow.

The solution is now complete with the wall temperature and bulk temperature available from Eqs. (11) and (12), respectively. In the following section, some representative results are presented.

Results and Discussion

Equations (11) and (12) are now used to generate results by direct numerical integration. The problem of interest is heat transfer to a fully turbulent flow in a smooth, round pipe with no source term ($S = 0$). The absence of a source term allows Eq. (13) to be used for the total heat transfer results.

The effects of the turbulent velocity profile $v(\eta)$ and eddy diffusivity $g(\eta)$ show up directly in the solution of the eigenvalue problem given by Eq. (16). As discussed in the Analysis section, this eigenvalue problem is solved by numerical integration. Table 1 shows the first five eigenvalues and eigenfunctions for 24 different combinations of the three parameters affecting the solution: H_o, Re, and Pr. As seen in Table 1, the eigenvalues climb more rapidly as Re and Pr increase. H_o does not affect the rate of growth of the eigenvalues, but it causes a positive shift of each eigenvalue as H_o increases. As usual, the normalized eigenfunctions evaluated at the wall alternate in sign and grow in absolute value as $m \to \infty$. The eigenfunctions also increase slightly in absolute value with an increase in Re and Pr but tend to zero as H_o tends to infinity. When $H_o = \infty$, the eigenvalues and eigenfunctions correspond to the constant wall temperature problem.

The numerical solution of the eigenvalue problem is the most computationally demanding part of the entire solution methodology. The maximum number of eigenvalues required was 60, which took 8 min of CPU time on an IBM 3090 to calculate. Therefore, it is beneficial to determine precisely how many eigenvalues are required. The Green's function given by Eq. (15) is the only place where the eigenvalues show up directly, so an analysis of the convergence rate of the Green's function determines how many eigenvalues are needed. The slowest rate of convergence occurs when $\xi - \xi_o$ is a minimum. Since the case $\xi - \xi_o = 0$ has been eliminated by the singularity subtraction employed in Eq. (11), the slowest convergence will occur when $\xi - \xi_o = \Delta\xi$. It seems that the convergence would be increasingly more difficult as Pe grows larger for a given value of $\Delta z/r_o$ since $\Delta\xi = \Delta z/r_o\,\mathrm{Pe}$. However, this is not the case since the eigenvalues grow much more rapidly as Pe gets large as shown in Table 1, thus offsetting the effect of smaller $\Delta\xi$. In fact, the required number of eigenvalues remains virtually constant for a given value of $\Delta z/r_o$. As $\Delta\xi$ gets larger while holding Re and Pr constant, experience shows that the number of terms required for convergence is proportional to $(\Delta\xi)^{-0.3}$.

In the solution of the integral equation given by Eq. (11), it is necessary to integrate from the tube inlet to the current axial location by steps of $\Delta\xi$. Although a marching-type solution could be employed, it is more convenient to integrate backwards from the current axial location towards the tube inlet and take advantage of the exponentially decaying nature of the Green's function. Since the wall temperatures far upstream from the current axial location cease to play a significant role in the solution, they can be neglected. This results in considerable savings in computer time and storage.

The integration technique chosen to solve Eq. (11) is the trapezoid rule. As demonstrated in Ref. 11, this method was found to give results indistinguishable from those using a finite-difference scheme[9] for laminar flow in a pipe. If higher accuracy is desired, a higher-order integration scheme could be implemented at the expense of greater computer time. Overall, the most important numerical parameter is the step size $\Delta\xi$ since it affects both the accuracy of the numerical integration of Eq. (11) and the convergence of the Green's function given by Eq. (15). The most numerically difficult case, requiring the smallest $\Delta\xi$, involves a stepwise periodic heat transfer coefficient which changes from relatively high to low values at a high frequency. The most difficult cases considered (Figs. 4 and 5) required $\Delta\xi \simeq 10^{-6}$ for 3 significant figures of accuracy in the wall temperature and 4 significant figures in the bulk temperature. However, $\Delta\xi \simeq 10^{-5}$ is sufficient for most cases as long as an abrupt change in $H(\xi)$ is not straddled. The bulk temperature, and hence $Q(\xi)$, can always be calculated more

Table 1 Eigenvalues and normalized eigenfunctions

		$H_o = 1$		$H_o = 5$		$H_o = 50$		$H_o = \infty$	
	m	λ_m	$\psi_m(1)$	λ_m	$\psi_m(1)$	λ_m	$\psi_m(1)$	λ_m	$\psi_m(1)$
Re = 5000	1	1.898	1.801	3.580	1.277	5.445	0.291	5.879	0.000
Pr = 0.7	2	16.886	−2.541	17.452	−1.907	18.586	−0.470	18.932	0.000
	3	28.279	3.629	29.005	2.851	30.644	0.741	31.166	0.000
	4	39.278	−4.228	40.038	−3.545	42.150	−1.042	42.911	0.000
	5	50.511	4.349	51.168	3.822	53.414	1.297	54.381	0.000
Re = 50,000	1	1.991	1.973	4.301	1.841	10.236	1.039	14.646	0.000
Pr = 0.7	2	43.651	−2.414	43.903	−2.282	45.514	−1.398	47.869	0.000
	3	75.252	3.125	75.498	2.967	77.136	1.866	79.724	0.000
	4	106.361	−3.734	106.611	−3.559	108.327	−2.294	111.210	0.000
	5	137.227	4.299	137.484	4.111	139.302	2.706	142.511	0.000
Re = 500,000	1	2.110	2.065	4.695	2.043	14.055	1.831	40.994	0.000
Pr = 0.7	2	130.267	−2.517	130.367	−2.496	131.386	−2.279	141.282	0.000
	3	224.125	3.233	224.222	3.208	225.208	2.946	235.608	0.000
	4	316.864	−3.810	316.959	−3.782	317.935	−3.493	328.941	0.000
	5	409.077	4.319	409.172	4.289	410.149	3.978	421.785	0.000
Re = 5000	1	1.950	1.900	3.977	1.580	7.380	0.543	8.637	0.000
Pr = 5.0	2	42.287	−3.356	42.727	−2.785	44.082	−0.934	44.740	0.000
	3	67.781	6.315	68.776	5.357	71.979	1.828	73.481	0.000
	4	91.015	−7.515	92.129	−6.755	96.708	−2.736	99.329	0.000
	5	116.704	7.453	117.584	6.892	121.910	3.208	124.979	0.000
Re = 50,000	1	2.003	1.997	4.424	1.947	12.368	1.521	25.045	0.000
Pr = 5.0	2	115.723	−2.487	115.828	−2.429	116.734	−1.928	120.132	0.000
	3	199.300	3.349	199.410	3.272	200.368	2.601	204.010	0.000
	4	281.312	−4.228	281.436	−4.131	282.520	−3.285	286.637	0.000
	5	362.345	5.217	362.491	5.097	363.773	4.049	368.584	0.000
Re = 500,000	1	2.361	2.068	5.272	2.062	16.405	1.997	86.827	0.000
Pr = 5.0	2	347.812	−2.528	347.859	−2.521	348.379	−2.449	365.462	0.000
	3	598.337	3.263	598.383	3.255	598.887	3.165	616.256	0.000
	4	845.798	−3.871	845.844	−3.862	846.346	−3.759	864.302	0.000
	5	1091.777	4.424	1091.824	4.414	1092.333	4.300	1110.026	0.000

accurately than the wall temperature under similar conditions.

Although the analysis is carried out in terms of the dimensionless axial distance ξ, the results which follow are presented as a function of z/r_o. This is done in order to make a meaningful parameter study of the effects of Re and Pr on the heat transfer characteristics in turbulent flow, since Re and Pr independently affect the temperature distribution. This is in contrast to the laminar flow case[11] where the effects of Re and Pr are completely absorbed in the axial variable ξ.

The external convection coefficient variations are shown in Fig. 1. A stepwise periodic variation is taken as the model for a tube fitted with an array of external fins. This is the same model used in Refs. 9–11 for the laminar flow case. The finned tube is modeled as an unfinned tube with a stepwise periodic variation of the convection coefficient, where a low H represents the unfinned region and a high H represents the enhancement of the heat transfer due to the fin. A harmonic variation is also chosen for comparison with the stepwise periodic case. This can be used to model the effect of axial heat conduction in the tube wall, which has a smoothing effect on the convection coefficient. For a valid comparison of results, the average of the harmonic variation has been adjusted to equal that of the stepwise periodic case while maintaining the minimums at the same value.

First, results for a constant heat transfer coefficient, $H(\xi) = H_o$, are presented. For this case, Eqs. (11) and (12) reduce to the exact analytical solutions since $K(\xi,\xi_o) = 0$. Figure 2 shows the effect of Re and the magnitude of the external convection coefficient on the Nusselt number, defined by Eq. (14). An increase in Re causes the internal convection coefficient or Nusselt number to increase because of a higher velocity near the wall and an increase of turbulent mixing in-

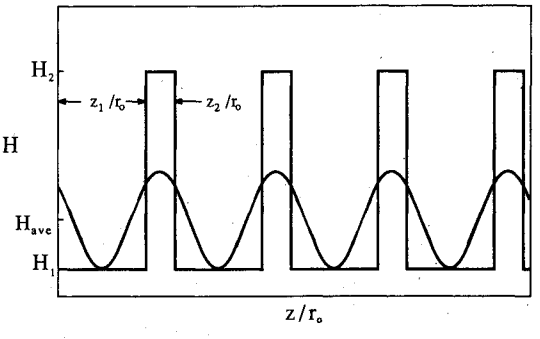

Fig. 1 External convection coefficient variations.

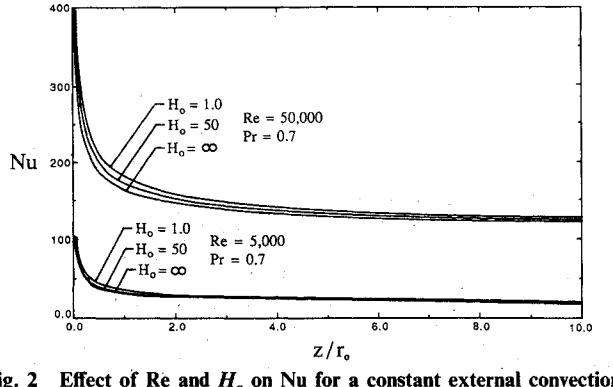

Fig. 2 Effect of Re and H_o on Nu for a constant external convection coefficient.

tensity. The effect of H_o is clearly very small with Nu dropping slightly as H_o increases. The $H_o = \infty$ case corresponds to a constant wall temperature and is the only case available for comparison with the literature. Comparing with the results presented by Notter and Sleicher[6] shows good agreement at both values of Re. Nu approaches its asymptotic limit very quickly for all cases in turbulent flow although an increase in Re increases the development length.

Figure 3 shows the effect of Pr on the Nusselt number. The trends displayed in Fig. 3 can be understood by examining the dimensionless eddy diffusivity obtained when the governing energy Eq. (5a) is rewritten in terms of z/r_o. After dividing Eq. (6g) by Re Pr, the total diffusivity is expressed as

$$\frac{g(\eta)}{\mathrm{Re\,Pr}} = \frac{1}{\mathrm{Re}}\left[\frac{1}{\mathrm{Pr}} + \frac{1}{\mathrm{Pr_t}}\frac{\varepsilon_m}{\nu}\right] \tag{18}$$

Here, it is clear that the radial heat transfer is made up of both a molecular diffusion term, represented by 1/Pr, and a turbulent mixing term, represented by $\varepsilon_m/\nu\ \mathrm{Pr_t}$, acting in parallel. Since the turbulent mixing term is only a function of Re, it is clear that as Pr becomes small, molecular diffusion will begin to dominate the turbulent mixing effect giving results similar to those for laminar flow. As Pr is increased, the turbulent heat transfer will dominate, except near the wall where the eddy diffusivity must vanish. Thus, for high Pr, the mixing effect produces a nearly uniform temperature profile in the central region of the pipe with a large temperature gradient near the wall where the molecular effects are important. As a result, Nu increases with Pr as shown in Fig. 3.

Figure 4 shows the effect of Re on the wall temperature for a stepwise periodic variation of H. In all cases, the wall temperature drops most quickly in regions of high H and rises in regions of low H due to an insulating effect in low H regions. However, the effect is much more pronounced at the lower Re since the lower fluid velocity near the wall allows more time for the heat transfer to affect the wall temperature. Another interesting point concerns the effect of greater mixing at higher Re. As Re increases, the wall temperature drops less steeply in regions of high H and climbs more rapidly in regions of low H due to the interaction with the hotter fluid near the center of the tube through greater turbulent mixing.

In Fig. 5, the effect of Pr on the wall temperature for a stepwise periodic variation of H is explored. At small Pr, the results appear similar to those of laminar flow because a large thermal diffusivity makes molecular effects important, as seen from Eq. (18). As Pr is increased, the effects of turbulent mixing begin to dominate the molecular diffusion and, consequently, the wall temperature is much higher in this case. As in Fig. 4, the wall temperature falls into a repetitive pattern with an ever-decreasing magnitude as heat is given up to the surroundings.

Figure 6 examines the effect of the external convection coefficient variation on the total heat transfer rate Q as defined by Eq. (13). In this case, both the stepwise periodic variation and the harmonic variation show considerable enhancement in the heat transfer rate over the constant H case, which represents an unfinned tube. The harmonic variation gives only slightly higher heat transfer than the stepwise periodic variation near the tube entrance. By about 50 pipe diameters, there is no appreciable difference in the heat transfer rate for the two variations. Thus, the exact variation of H is not as important in turbulent flow as it is in laminar flow.[11]

In Fig. 7, the effect of Re on the rate of heat transfer from the pipe is examined. The dimensionless total heat transfer, as defined by Eq. (13), decreases as the Re increases, which contradicts intuition. However, the total heat transfer, expressed in real variables, is proportional to $\mathrm{Re}\cdot Q$. If the results of Fig. 7 were plotted as $\mathrm{Re}\cdot Q$ vs z/r_o, the higher Re would give higher values of $\mathrm{Re}\cdot Q$, thus correlating with the expected trend. The lower Re flow approaches thermal saturation by 250 pipe diameters. A ten-fold increase in Re requires almost ten times the

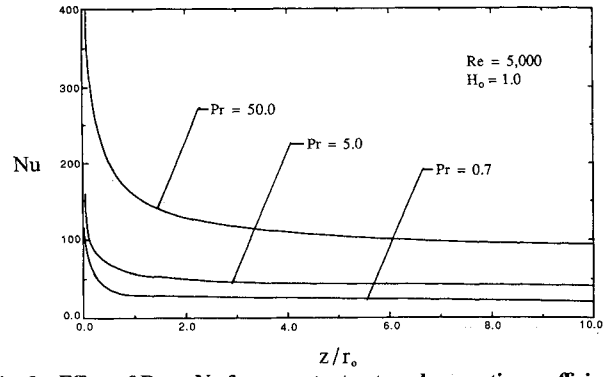

Fig. 3 Effect of Pr on Nu for a constant external convection coefficient.

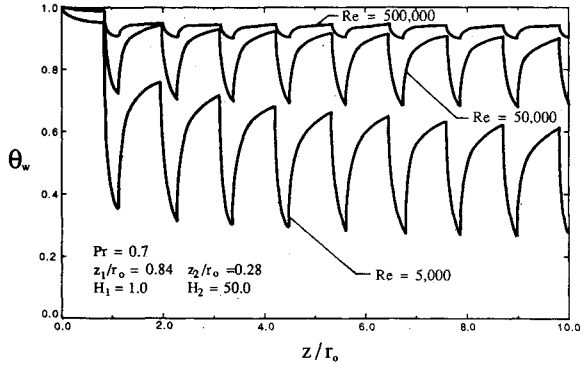

Fig. 4 Wall temperature results showing the effect of Re for a stepwise periodic heat transfer coefficient.

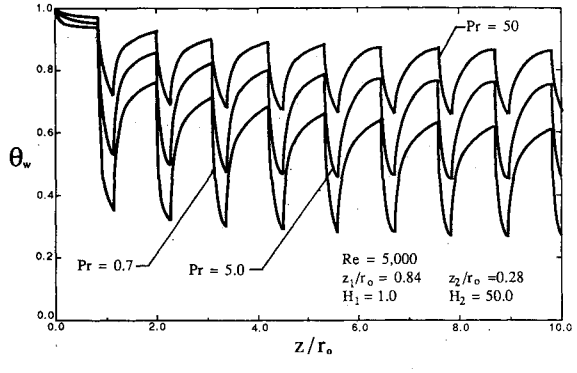

Fig. 5 Wall temperature results showing the effect of Pr for a stepwise periodic heat transfer coefficient.

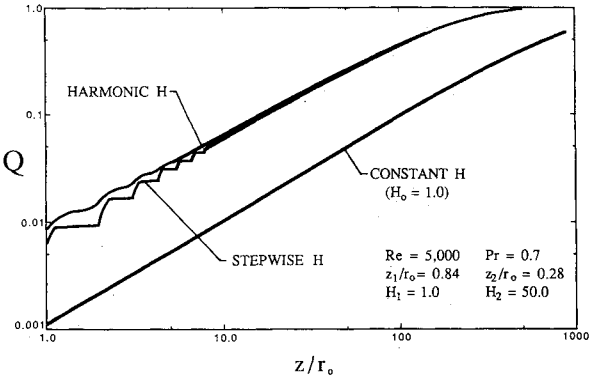

Fig. 6 Effect of external convection coefficient variations on the total heat transfer.

pipe length to achieve thermal saturation. The effect of greater mixing in the higher Re flows reduces the thermal resistance and allows the fluid to transfer heat faster to the wall, thus reducing the length of pipe required. The effect of Pr on the total heat transfer rate can be seen in Fig. 8. The total heat transfer increases as Pr is decreased due to an increase in the molecular portion of the total thermal diffusivity which lowers the thermal resistance to heat transfer across the fluid.

The effect of the flow model on the total heat transfer is examined in Fig. 9. It has been assumed that laminar flow can be maintained up to a Re of 4000. Hinze[15] (p. 707) reports that when particular care is taken, laminar flow can be maintained up to Re = 10^5. As expected, laminar flow provides the greatest resistance to heat transfer because of a low velocity near the wall and the absence of any mixing effects. Perhaps not so

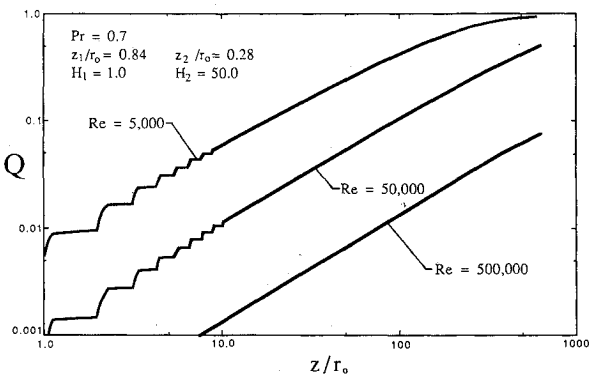

Fig. 7 Effect of Re on the total heat transfer for a stepwise periodic variation of the heat transfer coefficient.

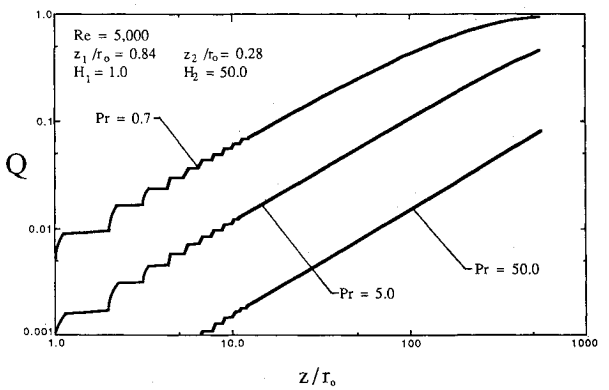

Fig. 8 Effect of Pr on the total heat transfer for a stepwise periodic variation of the heat transfer coefficient.

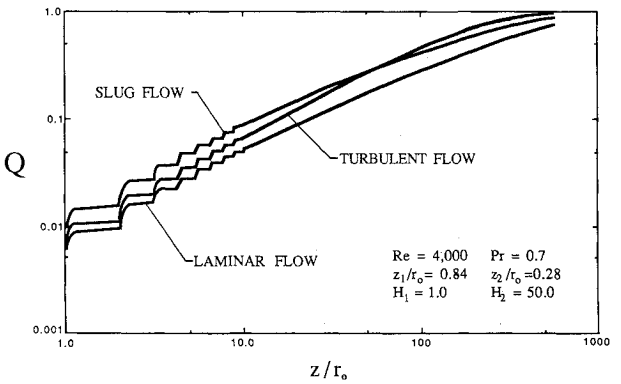

Fig. 9 Effect of flow models on the total heat transfer for a stepwise periodic variation of the heat transfer coefficient.

expected is the fact that slug flow gives higher heat transfer rates than turbulent flow up to about 30 diameters, after which turbulent flow achieves higher heat transfer rates. Apparently, the high velocity near the wall dominates the heat transfer characteristics when the bulk temperature is large. Eventually, however, the effect of turbulent mixing overtakes the effect of high wall velocity and the turbulent heat transfer becomes greater.

Summary and Conclusions

This investigation presents a solution methodology to solve the problem of fully developed turbulent pipe flow subjected to an axial variation of the heat transfer coefficient. The generalization to a variable heat transfer coefficient causes mathematical complexities due to the nonseparable nature of the problem. The solution technique uses a turbulent Green's function to transform the governing energy equation into a singular Volterra integral equation for the wall temperature. This integral equation is then resolved using the trapezoid rule with singularity subtraction.

Using the most complete turbulence model available for smooth pipe flow, results are presented showing the effect of Re and Pr on the wall temperature and heat transfer rate for both stepwise periodic and harmonic variations of the convection coefficient. In each case, higher Re and Pr results in higher wall temperatures and smaller heat transfer rates. The exact variation of the external convection coefficient does not appear to be critical as long as the average value remains the same. A comparison among turbulent, laminar, and slug flow models is also presented. Laminar flow has the highest internal resistance due to low velocity near the wall and the absence of turbulent mixing, thus gives the lowest total heat transfer. The slug flow model gives the highest heat transfer in the inlet of the pipe due to the high wall velocity; however, the heat transfer in the turbulent case eventually overtakes the slug flow case farther downstream due to turbulent mixing effects.

Overall, the solution technique has proven to be both accurate and economical, by combining the advantages of an analytical formulation with a simple numerical integration. The methodology itself is quite general and can handle a large class of problems with variable boundary condition parameters.

Acknowledgments

This work was supported by the National Science Foundation through Grant MEA-84-03964.

References

[1]Travis, J. R., Buhr, H. O., and Sesonske, A., "A Model for Velocity and Eddy Diffusivity Distributions in Fully Turbulent Pipe Flow," *Canadian Journal of Chemical Engineering*, Vol. 49, 1971, pp. 14–18.

[2]Martinelli, R. C., "Heat Transfer to Molten Metals," *Transactions of ASME*, Vol. 69, 1947, pp. 947–959.

[3]Sleicher, C. A. and Tribus, M., "Heat Transfer in a Pipe with Turbulent Flow and Arbitrary Wall Temperature Distribution," *Transactions of ASME*, Vol. 79, 1957, pp. 789–797.

[4]Sleicher, C. A., Notter, R. H., and Crippen, M. D., "A Solution to the Turbulent Graetz Problem by Matched Asymptotic Expansions — I: The Case of Uniform Wall Temperature," *Chemical Engineering Science*, Vol. 25, 1970, pp. 845–857.

[5]Notter, R. H. and Sleicher, C. A., "A Solution to the Turbulent Graetz Problem by Matched Asymptotic Expansions — II: The Case of Uniform Wall Heat Flux," *Chemical Engineering Science*, Vol. 26, 1971, pp. 559–565.

[6]Notter, R. H. and Sleicher, C. A., "A Solution to the Turbulent Graetz Problem — III: Fully Developed and Entry Region Heat Transfer Rates," *Chemical Engineering Science*, Vol. 27, 1972, pp. 2073–2093.

[7]Shibani, A. A. and Özisik, M. N., "A Solution to Heat Transfer in Turbulent Flow between Parallel Plates," *International Journal of Heat and Mass Transfer*, Vol. 20, 1977, pp. 565–573.

[8]Siegel, R. and Sparrow, E. M., "Turbulent Flow in a Circular Tube with Arbitrary Internal Heat Sources and Wall Heat Transfer," *Journal of Heat Transfer*, Vol. 81, 1959, pp. 280–290.

[9]Sparrow, E. M. and Charmchi, M., "Laminar Heat Transfer in an Externally Finned Circular Tube," *Journal of Heat Transfer*, Vol. 102, 1980, pp. 605–611.

[10]Vick, B. and Wells, R. G., "Laminar Flow with an Axially Varying Heat Transfer Coefficient," *International Journal of Heat and Mass Transfer*, Vol. 29, 1986, pp. 1881–1889.

[11]Vick, B., Beale, J. H., and Frankel, J. I., "Integral Equation Solution for Internal Flow Subjected to a Variable Heat Transfer Coefficient," *Journal of Heat Transfer*, Vol. 109, 1987, pp. 856–860.

[12]Riechardt, H. A., "Vollstandige Darstellung der Turbulenten Geschwindigkeitsverteilung in Glatten Leitungen," *ZAMM*, Vol. 31, 1951, pp. 208–219.

[13]Özisik, M. N., *Heat Conduction*, Wiley, New York, 1980.

[14]James, M. L., Smith, G. M., and Wolford, J. C., *Applied Numerical Methods for Digital Computation*, Harper and Row, New York, 1977.

[15]Hinze, J. O., *Turbulence*, McGraw-Hill, New York, 1975.